

Influence of Shear on Deformations of Coupling Beams

Andrew W. Fisher¹(✉), Michael P. Collins², and Evan C. Bentz²

¹ Read Jones and Christoffersen (RJC) Engineers, 144 Front St. W. #500,
Toronto, ON M5J 2L7, Canada
andrew@andrewfisher.ca

² Department of Civil Engineering, University of Toronto, 35 St. George Street,
Toronto, ON M5T 3L2, Canada
mpc@civ.utoronto.ca, bentz@ecf.utoronto.ca

Abstract. In the design of tall towers in Canada, the use of coupled shear walls is common where two or more tall walls are tied together by a series of relatively small, heavily loaded and short coupling beams. The stiffness of these coupling beams is important in determination of the distribution of forces throughout the structure and thus deserves study. This paper presents the results from a recent experiment on a coupling beam at the University of Toronto and describes the measured deformations in terms of components of the deformation. The results show that a flexure-only analysis would account for only 53% of the total predicted deformation. Addition of the effect of curvature resulting from shear (but not shear strain) increases the predicted percentage to 57% while, finally, inclusion of shear strains increases the percentage to 100%. This demonstrates that a flexure-only analysis will grossly underestimate the flexibility of such a member at service and ultimate limit state loads and shear strains must be included for accurate prediction of deformations. For a longer member that is more flexurally dominant, the respective contributions are 78% from flexure only, 85% from an analysis including curvature from flexure and shear (but not shear strain) and 100% from the combination of all three. Thus the contribution of shear-induced curvature can be more important for longer members than shorter ones.

Keywords: Shear · Stiffness · Coupling beams · Shear strains · Curvature

1 Introduction

In the design of tall buildings, a coupled shear wall configuration can provide an efficient structural system for lateral and gravity loading. In such systems a series of walls, potentially the full height of the building are tied together with relatively short, heavily loaded reinforced concrete beams. The larger the stiffness and shear capacity of these members, the more the pair of walls will be able to function as a single composite structural unit. As part of a study investigating the influence of side-cover spalling at ultimate limit states, a series of four full-scale coupling beams were tested at the University of Toronto. This paper will focus on the deformations observed for one of these specimens, CBF1. More details on this experiment as well as information about the other four can be found in the Master's thesis of the first author (Fisher 2016).

2 Experimental Program

The tests were performed in a specially designed rig to allow replacement of the coupling beam between different tests. Figure 1 shows the geometry and layout of the test setup while Fig. 2 shows the cross section of the specimen CBF1. As can be seen, the specimen is heavily reinforced in terms of both flexural and shear reinforcement. The setup compensates for self-weight and thus the member is subjected to approximately constant shear with a point of inflection at the middle of the span along the line of the vertical load application. The concrete strength at the date of testing was 80.3 MPa.

The results of the test were that the maximum force the member could resist was 1918 kN with flexural yield just starting to occur at the member ends at this peak load. As the deformations were increased beyond this point, however, the member failed in

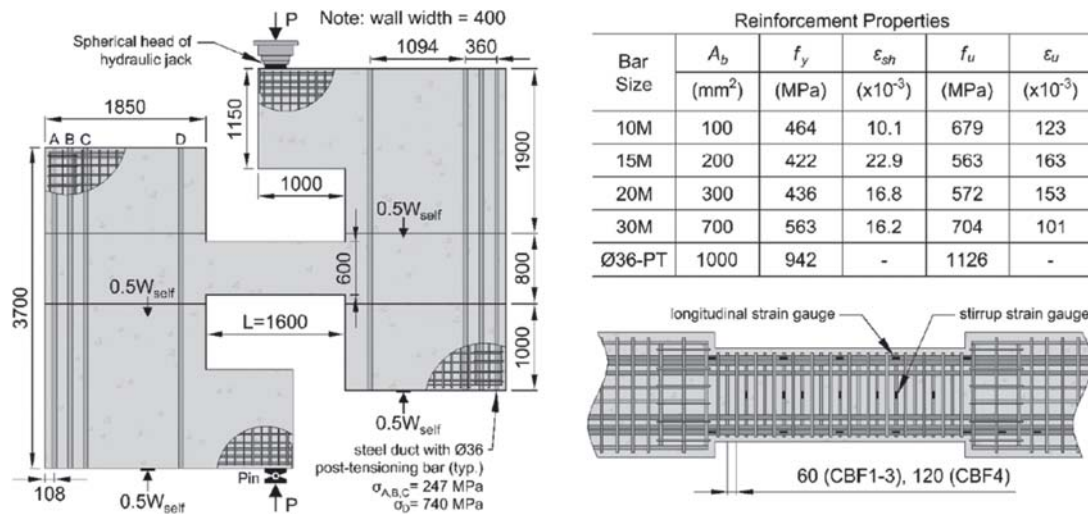


Fig. 1. Test setup

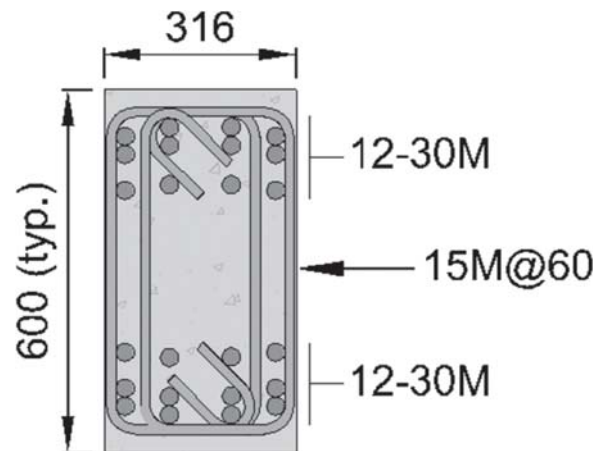


Fig. 2. Cross section of specimen CBF1

shear, though it was able to resist quite a significant shear force for displacements larger than that associated with the maximum shear force. Note that the member was intentionally strengthened in flexure from what the design code would require to ensure shear-critical behaviour. Figure 3 shows the pattern of cracks at the maximum load.

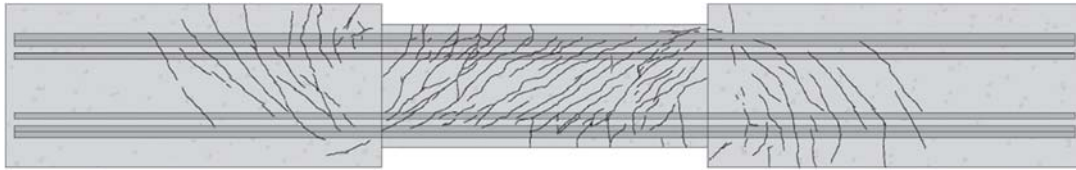


Fig. 3. Crack pattern of CBF1 at maximum applied load

The measured load-deflection relationship for this experiment up to the peak is shown in Fig. 4. For this graph the horizontal axis is Tangential displacement, the relative vertical displacement between each coupled shear wall.

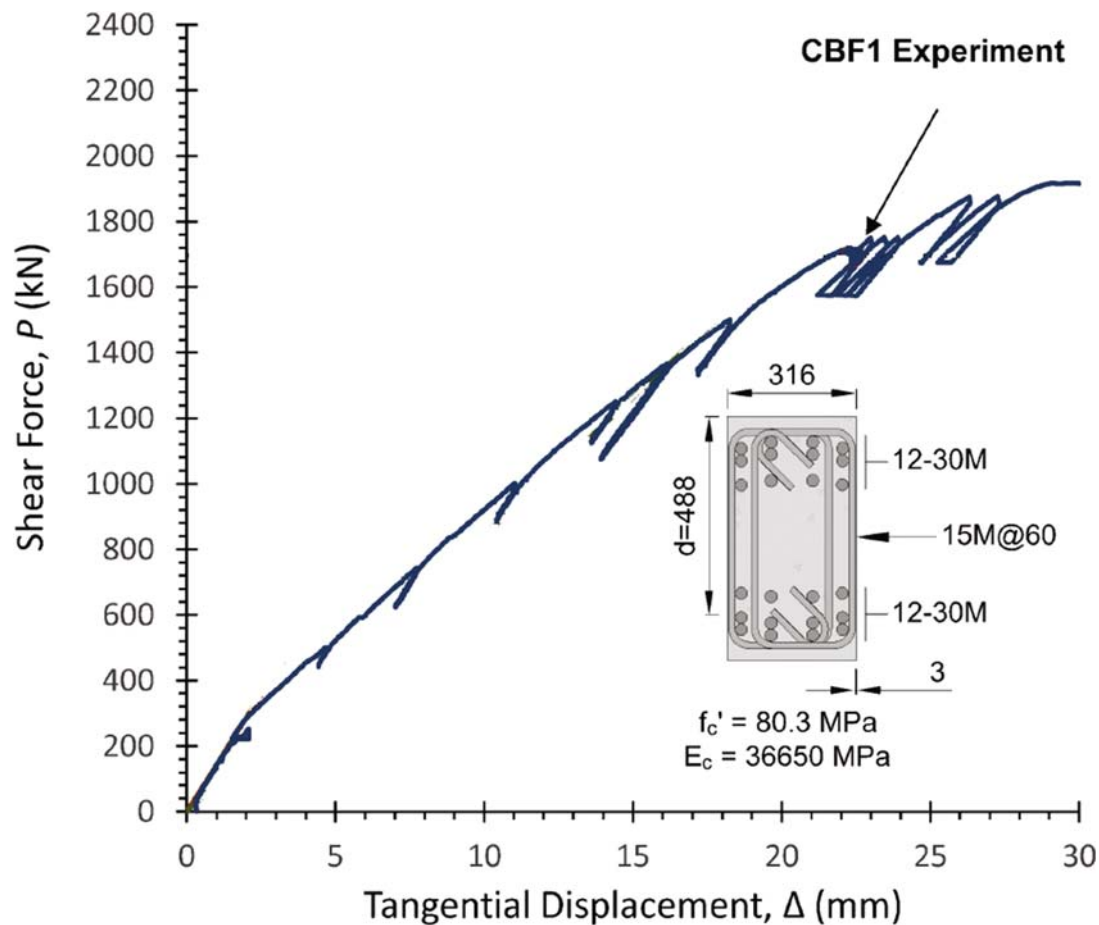


Fig. 4. Measured Load-Deformation Relationship

As the test progressed, detailed strain measurements were taken from strain gauges and Fig. 5 summarizes these results in terms of the longitudinal strains measured on the top layer of top steel and the bottom layer of bottom steel. In this figure LS stands for load stage. As can be seen tensile stresses are largest at locations where moments are the largest, but do not drop to zero at $X = 0$ where the moment is equal to zero. This will be discussed below.

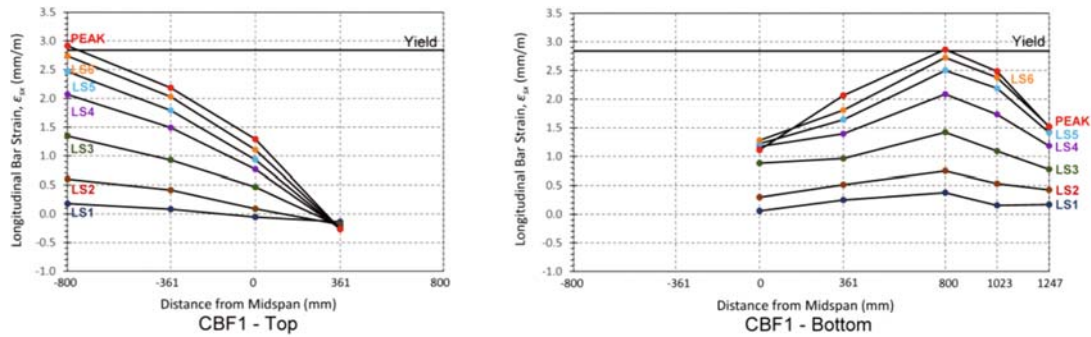


Fig. 5. Measured Longitudinal reinforcement strains on top of the member (left) and bottom of the member (right)

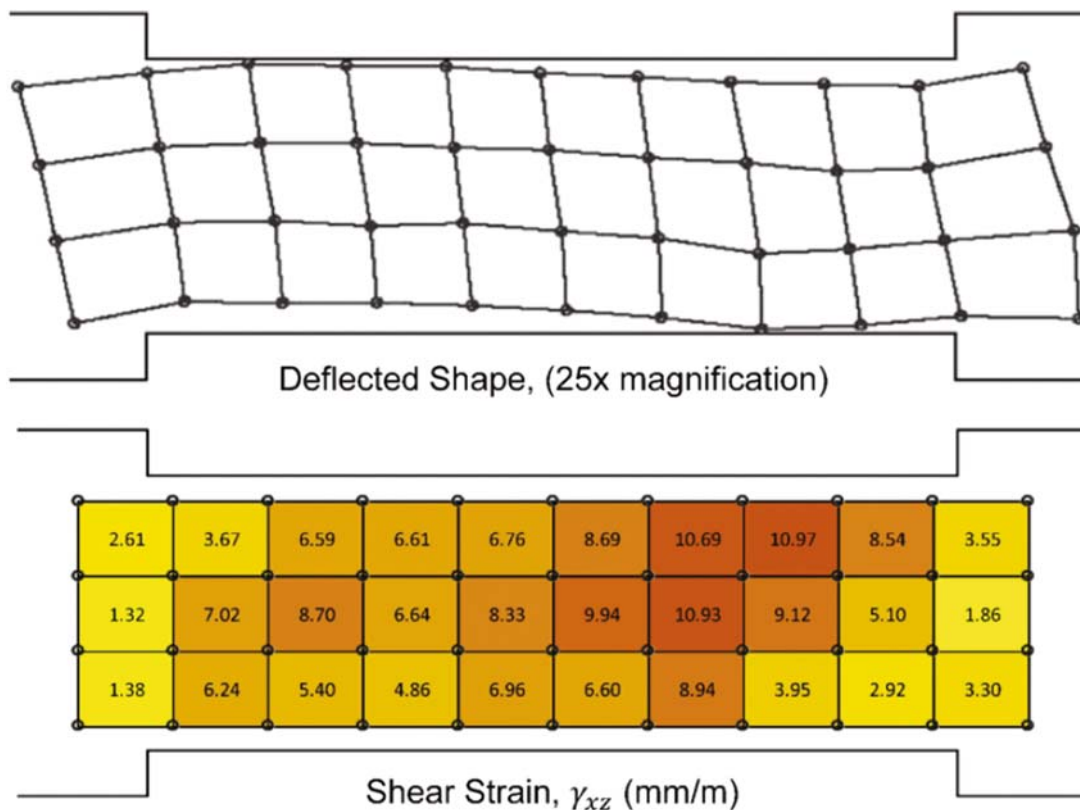


Fig. 6. Displaced shape and measured distribution of shear strains

The member displacements were measured by optically determining the coordinates of LED targets glued to the surface of the beam. Figure 6 shows the measured displaced shape as well as the distribution of shear strains in parts per thousand (mm/m).

3 Evaluation of Deformations

To understand the deformations of the member and, in effect, to transform the data in Figs. 5 and 6 into the displacements in Fig. 4, the concept of member curvature and shear strain will be used. That is, it will be assumed that plane sections remain plane. As the deformed vertical lines in the deflected shape shown in Fig. 6 are approximately straight, this assumption of engineering beam theory is appropriate.

To understand the strains, consider Fig. 7. On the left are the sectional force resultants: Moment (M_f) Shear (V_f) and Axial load (N_f). The section is assumed to carry shear by diagonal compression and, in this figure, by vertical component of prestress (V_p) though that term equals zero in the case of CBF1. These assumptions means that the sectional forces can be decomposed to the listed forces on the right side of the Free Body Diagram. Here it can be seen that the forces in the top and bottom flexural chord are dependent on the moment and axial load but also the longitudinal component of the diagonal compression. This explains why in Fig. 5 that even at the midspan where there is no moment or axial load, there remains a substantial axial strain on both the top and bottom chord.

If the flexural chord forces in Fig. 7 are translated to strains considering the reinforcement and, for compression, the compressive stiffness of the concrete, the longitudinal strains can be estimated. With the assumption of plane sections, the pattern of longitudinal strains shown is obtained. The curvature in the member may be determined as the slope of this line and also note that the mid-depth longitudinal strain, ϵ_x , is

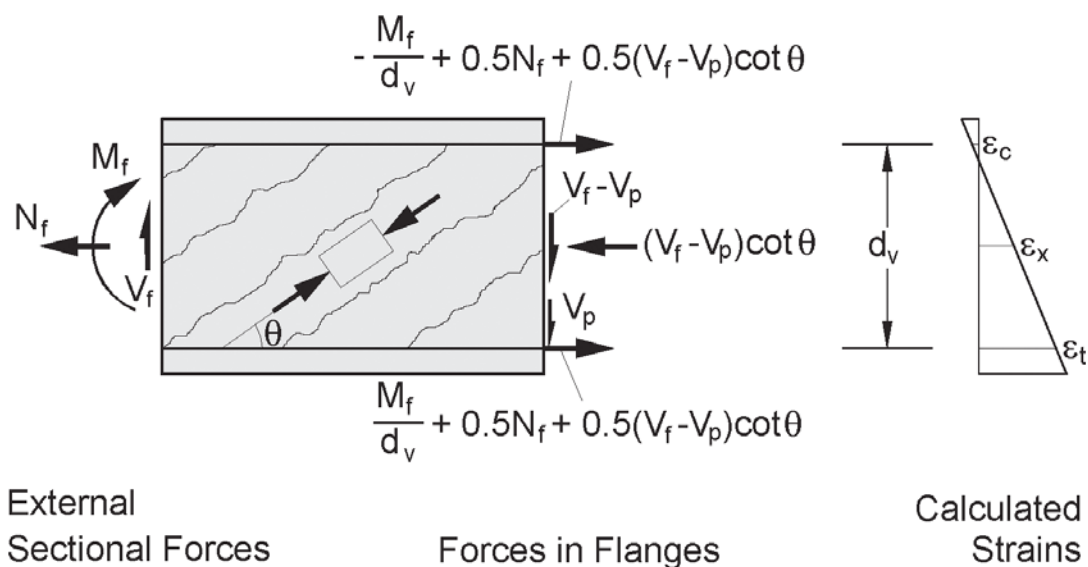


Fig. 7. Distribution of forces in web and flanges of section

approximately one half of the flexural tensile strain. This value of ϵ_x is used in the shear equations of the Model Code 2010 to determine shear strength (*fib* 2013). For shear strains, the shear forces can be converted to a shear stress and then it is possible to determine the shear strain using a general shear model such as the Modified Compression Field Theory (Vecchio and Collins 1986).

To determine overall deformations, the curvatures and shear strains must be integrated along the length of the member. In design it is often assumed that the curvature component of displacements will dominate and that the shear strains may be neglected. While this can be true, it is unclear if this will be a good assumption for short, heavily loaded members such as this.

More specifically, however, this simple model shows that there can be considered three parts to the deformation in total. The first is the curvature due to the flexural and axial load components of the applied loads in Fig. 7 alone, and these are well-known and predictable by a fibre-model for example. As noted the shear strains are another term that needs to be considered, but a third less-often considered contribution comes from the increase in curvature coming from shear. That is, since shear can be assumed to cause a longitudinal tensile force in the top and bottom flexural chord, and these chords have different axial stiffnesses (assuming the member is not cracked over the full depth), there will be a component of curvature that comes from the shear alone in a flexurally cracked member. It is of interest to know how important each of these three components are, one caused by moment and the other two by shear.

4 Response Analysis

To determine these components, the program Response has been used (Bentz 2016). This program, written by the third author calculates sectional responses based on the assumptions of plane sections remaining plane, that there is zero “clamping stress” through the thickness of the member, and that the MCFT provides good estimates of shear behavior. The analysis is similar to a fibre-model but considers biaxial behavior at each layer in the depth and the thickness of these layers is dynamically assigned to maximize precision and convergence stability. The shear stress profile is determined from first principles. The program allows multiple sections to be considered side-by-side along the length of the member and then integrated to produce load-deformation relationships as is desired in this case.

The predicted strength for member CBF1 from Response is 1880 kN with a tangential displacement of 23.1 mm which compares well with the observations in Fig. 4. The predicted crack diagram at failure is shown in Fig. 8 and also compares well with the observed pattern in Fig. 3.

Response automatically considers all three contributions to deformation that are explained in the section above. Given that the authors control this program, however, it is possible to “turn off” some of the components of deformations to see how influential they are for this experiment. Figure 9 shows the predicted load deformation relationships considering (A) only flexural strains with shear totally ignored, (B) considering curvature from moment as well as shear but neglecting shear strains and (C) all three strain components.

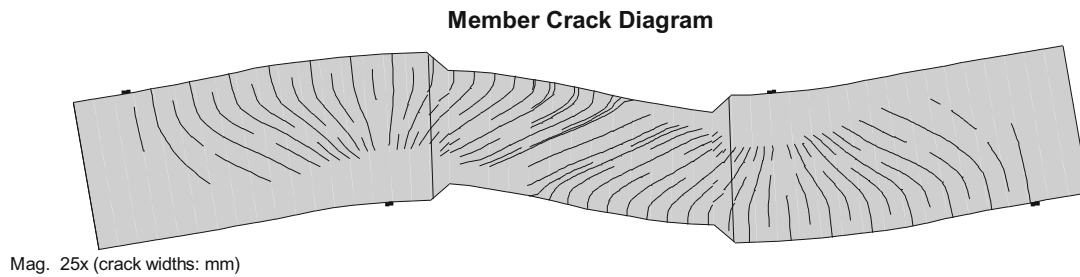


Fig. 8. Predicted Crack pattern at peak load by Response

Looking at Fig. 9, it can be seen that prior to flexural cracking the contribution of shear to displacements is negligible. The increase in deformations beyond those from flexure alone after cracking can be seen to increase with load and to be mostly caused by shear strain. With this short-span experiment, about 90% of the shear-induced deformations come from shear strain with the remainder from shear induced curvature. Note that since the member is predicted to fail in shear, the flexure-only calculation continues to higher loads than that for the other two cases as the member strength was limited by shear. Thus the nonlinearity in predicted deformation (Curve C) can be seen to result from increases in shear strain rather than curvature which can be expected for members with elastic flexural reinforcement.

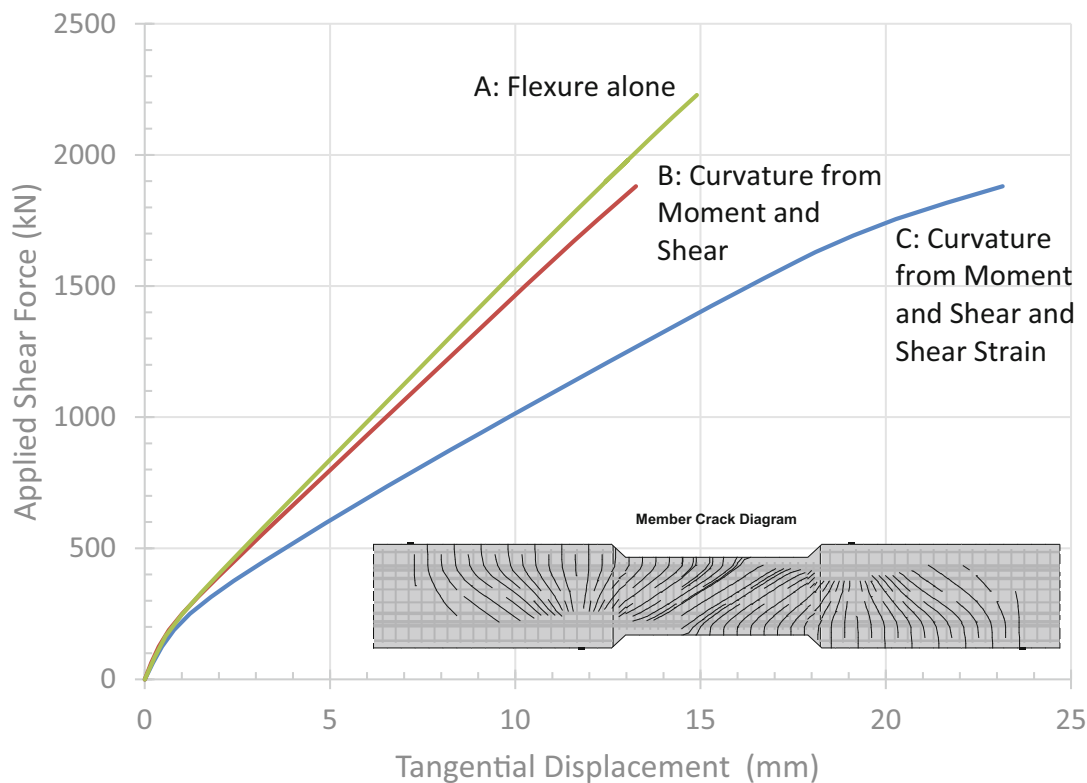


Fig. 9. Predicted Contributions to Deformation

At peak predicted load, the deformations from a flexure-only analysis contribute only about 53% of the deformations predicted when all three mechanisms are considered. If the contributions of shear to curvature are included, then the deformations increase to 57% of the total predicted deformations. Thus it can be concluded that for this analysis it is appropriate to ignore the curvature due to shear strain and consider only curvature due to flexure and shear strains to get a good prediction of overall behavior for short coupling beams.

If a similar analysis is done for the proportionally longer 4000 mm deep specimen tested in Toronto and presented in the proceedings of the Cape Town *fib* meeting in 2016 (Bentz and Collins 2016), the deformations from a flexure-only analysis represent 78% of the deformations predicted including all three contributions to deformations. If the curvatures due to shear are added but shear strains are not, that ratio increases to 85%. This means that for members that are longer and more flexurally dominant than coupling beams, about a third of the shear-induced deformation can result from shear-induced curvature and thus it would be unwise to ignore it, though the total contribution from shear remains relatively small compared to that of a short coupling beam such as CBF1.

5 Conclusions

This paper presented the results of an experiment on a short coupling beam. For this experiment it was shown that neglecting the effects on shear on deformations will result in the deformations being underestimated by a factor of about two. The majority of those additional deformations were predicted to be due to shear strain rather than the contribution of shear induced curvature. For longer members the shear deformations are less important though the contribution from shear-induced curvature is proportionally larger.

It is therefore appropriate to consider shear deformations in stiffness estimates of coupling beams though the specific contribution of shear induced curvature may be neglected with only a small cost in accuracy. For longer members that are more flexurally dominant, shear contributes a smaller, though still relevant additional deformation with shear-induced curvature being a larger fraction than for coupling beams.

References

- Fisher, A.W.: Shear performance of heavily reinforced high-strength concrete coupling beams. MASc thesis. Department of Civil Engineering, University of Toronto (2016). 286 pp.
- fib: The fib Model Code for Concrete Structures 2010, fib, Geneva (2013)
- Bentz, E.C., Collins, M.P.: A four metre deep shear test: comparing international predictions to observations. In: Proceedings of fib 2016 Conference in Cape Town (2016). 7 pp.
- Bentz, E.C.: Response website, 24 December 2016. <http://www.ecf.utoronto.ca/~bentz/r2k.htm>
- Vecchio, F.J., Collins, M.P.: The modified compression field theory for reinforced concrete elements subjected to shear. ACI J. **83**(2), 219–231 (1986)